

CALIBRATION OF SPECTROMETRIC DETECTORS FOR AIR KERMA RATES IN ENVIRONMENTAL MONITORING

by

Marcel OHERA^{1*}, Daniel SAS², and Petr SLADEK³

¹ National Radiation Protection Institute, Prague, Czech Republic

² NBC Defence Institute, University of Defence, Vyškov, Czech Republic

³ IAEA, Nuclear Science and Instrumentation Laboratory, Seibersdorf, Austria

Scientific paper

<https://doi.org/10.2298/NTRP2004323O>

The spectrometric systems, especially based on NaI(Tl) and HPGe detectors, are used for nuclide identification and calculation of their activities from the ground measurements and air-borne monitoring. The determination of the air kerma (dose) rates is also very important for environmental measurements. In such cases, the detectors should be calibrated for air kerma (dose) rates in nGyh^{-1} or μGyh^{-1} . A simple calibration of NaI(Tl), HPGe as well as plastic detectors for the low-level air kerma rates is presented in this contribution. This calibration is based on comparing the relative absorbed energy rate in detectors (MeVs^{-1}) calculated from spectra with the air kerma rates calculated by the Monte Carlo simulation and supplementary to the data from the RSS Reuter&Stokes high pressure ion chamber. This method also eliminates the conversion from the non-air kerma rates in crystals to the air kerma rates. Three different types of small cylindrical detectors were calibrated for the air kerma rates from the background of 26 nGyh^{-1} to some tens of μGyh^{-1} in the energy range to the maximum of 3 MeV. The results of calibrations of the 3" 3" NaI(Tl), HPGe detector and a small plastic detector (made of polystyrene) including some examples of environmental measurements are presented.

Key words: air kerma rate calibration, NaI(Tl), HPGe and plastic detector, Monte Carlo simulation

INTRODUCTION

Many papers have been devoted to NaI(Tl) and HPGe spectrometric detector calibration, especially determination of their efficiencies, for example in [1, 2]. The determination of the air kerma rates was also described for NaI(Tl) detectors in many publications, [3-6] and others.

Beck *et al.* [3, 4] have shown, with their spectrometric methods using NaI(Tl) crystals, that the total energy absorbed in the crystal, ranging from 0.15 MeV to 3.4 MeV, is closely proportional to the total dose rate determined with a high pressure ion chamber in various field locations. Moreover, for purposes of determining the contributions of natural and man-made gamma-ray emitters to the total terrestrial exposure-dose-rate, they introduced the conversion factors. The factors were determined for each gamma peak individually.

The experimental method [5] converted information deposited in gamma spectra from a 3" 3" NaI(Tl) crystal with dimensions of 7.6 cm x 7.6 cm to the air kerma rate. The calibration procedure was based on the measurements of energy deposited in a detector using 10

radioactive sources with well-known activity in an energy range from 60 keV to 1836 keV. For different kinds of radioactive sources, the spectra for different angular positions were acquired with respect to the longitudinal axis of the detector. The spectra were acquired for different types of radioactive sources and different angular positions with respect to the longitudinal axis of the detector. The total energy which was deposited in the detector was also calculated by the Monte Carlo calculations. The calibration factors for each from 10 energy areas were calculated based on well-known air kerma rates from the sources. The calibration procedure was verified by comparing results using ^{137}Cs and ^{60}Co collimated beams and the calibrated high pressure ion chambers.

The paper [6] describes the method of air dose rate determination in a 3" 3" NaI(Tl) crystal. Two quantities, *i. e.*, absorbed energy rate and average absorbed energy in a 3" 3" NaI(Tl) crystal were determined. The crystal response was corrected by the conversion factors which were determined as a function of the average gamma energy represented by gamma energy in a place to be measured and which can be obtained by the measurement of average absorbed energy.

* Corresponding author; e-mail: marcel.ohera@suro.cz

Other sophisticated methods of air kerma rate calculation based on the conversion factors between the non-air kerma rate in the detector and the air kerma rate were presented in [7-9]. These methods are applicable to environmental and airborne measurements.

The calibration procedure described in this contribution eliminates both the energy dependence of nuclides used for calibration and the non-air-kerma rate to air kerma rate conversion in the detectors used. On the other hand, the method is partly limited. It is not suitable for the nuclides with lower gamma energies only such as ²⁴¹Am, ⁵⁷Co, ¹³³Ba, etc. (energy below 300 keV).

We primarily modified previously described methods [5, 6] according to our available means. The proposed calibration method was successfully applied for calibrating both small cylindrical NaI(Tl) detectors, HPGe detectors and even small cylindrical plastic detectors. All detectors had small volumes (<1000 cm³) and the ratio of diameter/length was about 1.0. Some examples of environmental measurements are also presented.

THEORY

The air kerma rates determined from total cps are energy dependent. Figure 1 shows the relationship between cps (counts per second) and the air kerma rates K_a for three different nuclides (¹³⁷Cs, ¹⁵²Eu, and ⁶⁰Co) in a 3" x 3" NaI(Tl) detector (AGRS Pico Envirotec, Inc.). We defined the relative absorption energy rate E_{ma} based on the output spectrum to eliminate this effect.

The relative absorption energy rate E_{ma} in a crystal was determined as

$$E_{ma} = \frac{\int E_a N(E_a) dE_a}{t} \quad (1)$$

where E_{ma} is the relative absorption energy rate in the crystal in MeV per second, the value of E_a is energy in MeV in the interval dE_a , and $N(E_a)$ are the number of

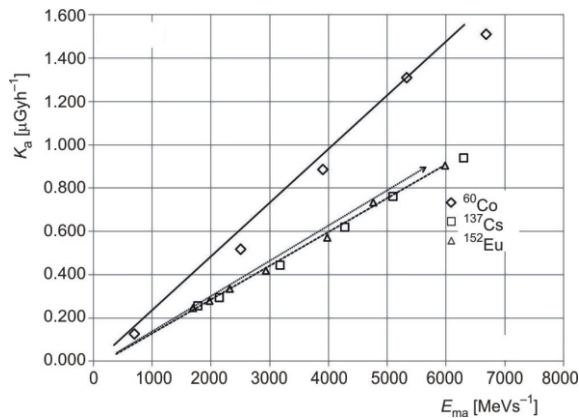


Figure 1. Example of the air kerma rate vs. total cps for ¹³⁷Cs, ⁶⁰Co, and ¹⁵²Eu measured in the 3" x 3" NaI(Tl) detector

counts corresponding to E_a in the interval $E_a, E_a + dE_a$ and t is the life (real) time in seconds.

Because multi-channel analysers were always used, then the aforementioned formula can be modified accordingly

$$E_{ma} = \frac{\sum_{j=i}^n E_a N(E_a)}{t} \quad (2)$$

where E_{ma} [MeVs⁻¹] is the relative absorption energy rate, t – the live (real) time, j – the initial channel number and n – the final channel number and $N(E_a)$ is the number of counts with an energy E_a in the interval $E_a, E_a + \Delta E_a$ in a channel over the measuring time t .

The E_{ma} value can be calculated from the energy calibrated spectra. Based on the spectra measured in NaI(Tl) detectors, HPGe or plastic detectors the air kerma rates should be determined in the place of the detector (on condition that kerma is equal to dose).

We assumed according to [3] and [4] that the relative absorbed energy, respectively the relative absorbed energy rate E_{ma} in MeVs⁻¹ characterized by the output energy spectrum, is closely proportional to the air kerma rate K_a in the place of the detector.

When calibrating a detector, we needed a set of pairs of relative absorbed energy rates E_{ma} and air kerma rates K_a in the required range of air kerma rates to determine the relationship between both quantities

$$K_a = f(E_{ma}) = f \left(\frac{\sum_{j=i}^n E_a N(E_a)}{t} \right) \quad (3)$$

In the Monte Carlo simulation, the detector volume in question was replaced by the air and the air kerma rates were calculated for specific source-detector distances. This approach is more appropriate because we could simulate the detector volume more precisely. The reference measurement system can also be used if the Monte Carlo simulation is not available. In such case, for example, the RSS Reuter&Stokes high pressure ion chamber can be used.

In case of the RSS high pressure ion chamber, the exposure rate¹ X was measured in the traditional unit Rh⁻¹. Therefore, all data were converted to SI units, in our case to the air kerma rate K_a in μGyh⁻¹. The following conversion formulae were applied to convert the exposure rate X to the air kerma rate K_a .

$$\frac{X}{K_a} = 2.95 \cdot 10^{-2} \frac{\text{Ckg}^{-1} \text{h}^{-1}}{\text{Gyh}^{-1}} = 114.5 \frac{\text{Rh}^{-1}}{\text{Gyh}^{-1}} \quad (4)$$

¹ Obsolete dosimetric quantity defined as the exposure dX/dt is the quotient of dX by dt , where dX is the increment of exposure in the time interval dt

$$\frac{K_a}{X} = 33.85 \frac{\text{Gyh}^{-1}}{\text{Ckg}^{-1}\text{h}^{-1}} \quad 8.73 \cdot 10^3 \frac{\text{Gyh}^{-1}}{\text{Rh}^{-1}} \quad (5)$$

Finally, the regression curves were calculated for the pairs of air kerma rates K_a vs. the relative absorbed energy rates E_{ma} for the appropriate energy range

$$K_a = A_1 + A_2 E_{ma} + A_3 (E_{ma})^2 + A_4 (E_{ma})^3 \quad (6)$$

MATERIALS AND METHODS

Calibration rooms

The detectors were usually calibrated from 0.026 μGyh^{-1} to some 0.15 μGyh^{-1} (in some cases up to 3 μGyh^{-1}) in the low-background chamber (hereinafter referred to as the LBC chamber) at the National Radiation Protection Institute in Prague (hereinafter referred to as SURO). This chamber is routinely used for the whole-body counting of the internally contaminated persons.

The chamber is made from special low-background material made of steel plates with a thickness of 3 × 6 cm plus 3 cm steel free of man-made nuclides, in total 21 cm steel with an extremely low natural nuclide contents. The complete inner surface is covered with copper with a thickness of 1 mm. The inner dimensions of the chamber are 248 cm × 201 cm × 200 cm (D × W × H). The background inside the LBC chamber achieves 26 nGyh⁻¹ [10].

All other measurements and calibrations for higher air kerma rates were performed at the calibration room of the NBC Defence Institute, University of Defence in Vršov, CZ which offered the experimental area of approximately 4 m × 10 m.

This area allowed exposing the detectors from a natural background of 0.125 μGyh^{-1} to 65 μGyh^{-1} depending on the source-detector distances used from 2.0 up to 8.0 m and the sources used.

Sources

The low-activity ¹⁵²Eu, ⁶⁰Co, and ¹³⁷Cs sources produced by the Czech Metrological Institute (activities in a range of hundreds kBq) were applied in the low-background chamber for calibration.

The sources of ¹⁵²Eu (50.2 MBq), ⁶⁰Co (100 MBq, 500 MBq and 2 GBq), ²²⁶Ra (175 MBq) and ¹³⁷Cs (102.1 MBq, 455.1 MBq and 3.145 GBq) were used in the NBC calibration room to achieve the air kerma rates up to 65 μGyh^{-1} .

Reuter&Stokes high pressure ion chamber

The RSS Reuter&Stokes high pressure ion chambers were also used to compare the results from

the simulation. The Reuter&Stokes high pressure ion chambers RSS-112 or RSS-131 were utilized in our experiments while the RSS-112 chamber was certificated by the Czech Metrological Institute, Certificate No. 9051-PS-8541-12. These devices use high pressure chambers with a volume of 7.9 litres. The measuring range is from approximately 2 μRh^{-1} to 10 Rh^{-1} . It is nearly independent in an energy range from 0.07 to 10 MeV. The chamber is not sensitive to electrons (beta). Exposure rates X in Rh^{-1} coming from the RSS were transformed into air kerma rates K_a in nGyh^{-1} .

Detectors and analyzers

The air-kerma rate calibration of the three different types of detectors is presented: 3" × 3" NaI(Tl) (Saint Gobain Crystals), HPGe GEM100P4-95 (ORTEC) portable semiconductor detector with a crystal dimension of 81.6 mm × 76.7 mm (D × L), relative efficiency of 100 %, and SPD plastic detector (NUVIA, CZ) 90 mm × 90 mm (D × L) based on polystyrene (C₈H₈)_n, 92.2 % C and 7.8 % H, with a density of 1.03 gcm⁻³. All detectors presented in this paper had a ratio of D/L near to 1.0.

The AGRS Spectrometer (Pico Envirotec, Inc. Canada) with a resolution of 512 channels and energy range adjusted from 35 keV up to 3.0 MeV was used in configuration with a 3" × 3" NaI(Tl). This spectrometer provides an automatically real time stabilized spectrum based on the peak of ⁴⁰K (1.46 MeV) and ²⁰⁸Tl (2.61 MeV).

The semiconductor detector ORTEC GEM100P4-95 (100 % efficiency, resolution of 2.0 keV at 1.33 MeV) was operated with digiDART ORTEC MCB. The HPGe detector was calibrated in an energy range from 35 keV to 3.008 MeV.

Finally, a 90 mm × 90 mm SPD plastic detector was also operated both with an AGRS spectrometer (Pico Envirotec, Inc. Canada) and ORTEC digiBASE. The energy calibration of the SPD plastic detector was based on determining the Compton maximum and Compton edges according to [11].

Monte Carlo simulation

The MCNP 6.1 code was applied, which is a general purpose Monte Carlo radiation transport code developed at the Los Alamos National Laboratory, and which was used to calculate the air kerma rates in the different source-detector positions in both the NBC calibration room and LBC chamber and for the different types of ionizing radiation sources.

The Tallies 6 (air kerma) and Tallies 8 (spectra) were calculated in the Monte Carlo simulation [12].

RESULTS AND DISCUSSION

The sets of pairs E_{ma} and K_a were established from the Monte Carlo simulation and from comparative measurements with a RSS high pressure ion chamber for ^{137}Cs , ^{60}Co , ^{226}Ra , and ^{152}Eu for different detector-source distances and activities.

The polynomial functions (3) describing the fitted correlation function between the relative absorbed energy rate E_{ma} and air kerma rate K_a were calculated by the LinRegGUI software (NUVIA, CZ).

Figure 2 shows the air kerma rates vs. distances for ^{137}Cs 102.1 MBq calculated by the Monte Carlo simulation and measured by the RSS chamber. Similar curves were measured and calculated for other nuclides ^{137}Cs , ^{60}Co , ^{226}Ra , and ^{152}Eu and their different activities.

Comparison of air kerma rates from the RSS high pressure ion chamber and MCNP calculation for ^{137}Cs with 455 MBq reference activity is shown in tab. 1.

The relationships of E_{ma} vs. K_a for the three above mentioned detectors, their settings and other parameters are given in tab. 2 and their calibration curves are shown in fig. 3.

This approach worked quite well for available wide-energy range nuclides (e. g., natural nuclides,

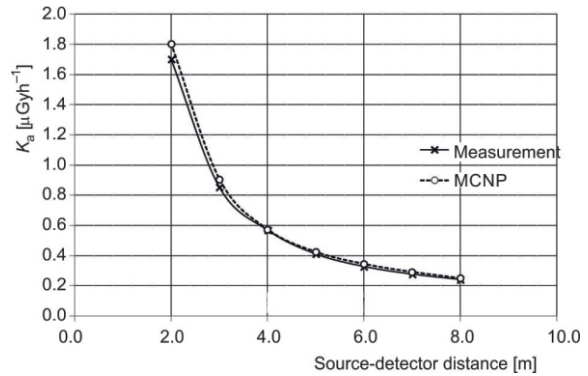


Figure 2. The RSS air dose rate measurements and MCNP air dose rate calculation for ^{137}Cs with a reference activity of 102.1 MBq in the NBC calibration room

^{152}Eu) and high energy nuclides (e. g., ^{137}Cs , ^{60}Co , etc.). Low energy nuclides were not available for calibrations.

Additionally, for ^{137}Cs , ^{60}Co , ^{226}Ra , and ^{152}Eu , the relationship of the air kerma rates K_a and the relative absorbed energy rates E_{ma} was also calculated for other nuclides, e. g. ^{241}Am , ^{57}Co , ^{131}I , etc. The results based on the Monte Carlo simulation in the NBC calibration room for the 3" 3" NaI(Tl) detector compared with measurements are also presented in fig. 4. It

Table 1. Exposure rates X , air kerma rates K_a and their uncertainties for ^{137}Cs 455.1 MBq measured in the NBC calibration room and calculated by the Monte Carlo simulation for different detector-source distances

Distance [m]	RSS high pressure ion chamber				MCNP		Differences between RSS and MCNP air kerma rates [%]
	X [Rh^{-1}]	X [Rh^{-1}]	K_a [nGyh^{-1}]	K_a [%]	K_a [nGyh^{-1}]	K_a [nGyh^{-1}]	
7.50	$9.06 \cdot 10^{-5}$	$4.0 \cdot 10^{-7}$	791	0.4	771	0.5	2.6
6.50	$1.08 \cdot 10^{-4}$	$2.0 \cdot 10^{-6}$	944	2.0	975	0.6	-3.2
6.00	$1.23 \cdot 10^{-4}$	$7.0 \cdot 10^{-7}$	1071	0.6	1100	0.5	-2.6
5.00	$1.66 \cdot 10^{-4}$	$5.0 \cdot 10^{-7}$	1453	0.3	1452	0.6	0.1
4.00	$2.44 \cdot 10^{-4}$	$1.0 \cdot 10^{-6}$	2128	0.4	2109	0.7	0.9
3.00	$4.01 \cdot 10^{-4}$	$1.5 \cdot 10^{-6}$	3504	0.4	3576	0.7	-2.0
2.50	$5.54 \cdot 10^{-4}$	$1.4 \cdot 10^{-6}$	4833	0.3	5029	0.8	-3.9
2.00	$8.30 \cdot 10^{-4}$	$2.0 \cdot 10^{-6}$	7246	0.3	7519	± 0.8	-3.6

Table 2. Main calibration features of NaI(Tl), HPGc, and SPD plastic detectors

Detector type	3" 3" NaI(Tl)	Ortec HPGc GEM100P4-95 S/N 50-TP50739A (efficiency 100 %)	SPD 90 mm 90 mm plastic detector
Analysers/resolution	Pico Envirotec Inc. AGRS /512 channels	ORTEC digiDART / 8192 channels	ORTEC digiBASE / 1024 channels
Radiation beam direction	Alongside the longitudinal detector axis, angular dependence is tested and is insignificant	Alongside the longitudinal detector axis, angular dependence is tested and is insignificant	Alongside the longitudinal detector axis, angular dependence is tested and is insignificant
Energy range	20 keV to 3 MeV	40 keV to 3.008 MeV	20 keV to 2.4 MeV
Air kerma rate K_a – calibration range	$0.026 \mu\text{Gyh}^{-1}$ to $30 \mu\text{Gyh}^{-1}$ ($DT_{\text{max}} \sim \text{N/A}$)	$0.026 \mu\text{Gyh}^{-1}$ to $1.5 \mu\text{Gyh}^{-1}$ ($DT_{\text{max}} \sim 15 \%$)	$0.026 \mu\text{Gyh}^{-1}$ to $17 \mu\text{Gyh}^{-1}$ ($DT_{\text{max}} \sim 4.5 \%$)
Relative absorbed energy rate E_{ma}	5 MeVs^{-1} to 56500 MeVs^{-1}	2.0 MeVs^{-1} to 3200 MeVs^{-1}	4 MeVs^{-1} to 21300 MeVs^{-1}
Total counts per second	15 cps to 160000 cps	Up to 7800 cps	13 cps to 42000 cps
Calibration equation K_a [μGyh^{-1}]	$K_a = 2.095 \cdot 10^{-2} + 4.7141 \cdot 10^{-4} E_{ma} + 4.1934 \cdot 10^{-9} (E_{ma})^2 - 6.4 \cdot 10^{-14} (E_{ma})^3$	$K_a = -6.465 \cdot 10^{-2} + 5.729 \cdot 10^{-4} E_{ma} - 3.247 \cdot 10^{-8} (E_{ma})^2$	$K_a = 2.2719 \cdot 10^{-2} + 8.3965 \cdot 10^{-4} E_{ma} - 6.0469 \cdot 10^{-9} (E_{ma})^2 - 1.1 \cdot 10^{-13} (E_{ma})^3$
Uncertainty of calibration	-5.4 % to +4.7 %	-3.3 % to +3.7 %	7.3 %

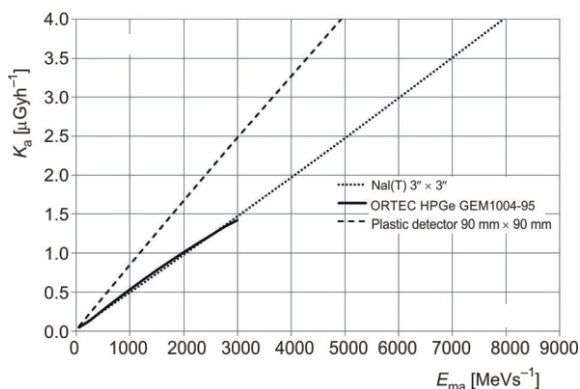


Figure 3. Detail on the calibration curves K_a in $\mu\text{Gy h}^{-1}$ vs. E_{ma} in MeVs^{-1} for NaI(Tl) 3" × 3", ORTEC HPGe GEM1004-95 and plastic 90 × 90 mm detector based on measurements in the LBC chamber and NBC calibration room

seemed that the approach described above does not work properly for the nuclides only with low gamma energies.

In the next steps, we focused on the verification of the calibration approach with wide energy ranges and high gamma energy. The spectra calculated in the Monte Carlo simulation in different conditions were also used.

The separate models of NaI(Tl) and HPGe detectors were also compiled in the Monte Carlo code. The documentation of the Engineering Sales Drawing delivered by the Saint Gobain producer was used to construct the model of scintillation of the 3" × 3" NaI(Tl) detector. Additionally, based on the basic data sheet information, many X-ray pictures were taken to specify the inner dimension of the ORTEC HPGe GEM100P4-95 detector, see fig. 5. Both detector models in the MCNP6.1 code were verified using different point sources. The simulation models of the NBC calibration room and the LBC chamber at SÚRO were also compiled in the Monte Carlo code with all accessories.



Figure 5. The X-ray picture of the ORTEC GEM100P4-95 HPGe detector

Plastic detectors were not simulated in the Monte Carlo code due to poor spectroscopic features and hence difficult GEB calculation [12].

Additionally, for Tallies 6 [12] used in the standard calibrations, Tallies 8 [12] in the Monte Carlo simulation giving spectra deposited in the individual tested detectors were calculated. Furthermore, the contribution of natural nuclides contained in the surrounding walls at the NBC calibration room was involved into the calculation. Simulated spectra were transformed to the relative absorbed energy rate E_{ma} in the GAMWIN (NUVIA, CZ) spectroscopy software [13] and the relationships of the air kerma rates versus the relative absorbed energy rates were calculated for comparison based on the eq. (3). It was proved in many cases that the proposed approach works well for the specific high gamma radiation. The 2" × 2" NaI(Tl) detector calibration is an example of such verification, see below.

This methodology has been applied to the calibration of many other NaI(Tl) detectors with different small volumes, HPGe detectors as well as some

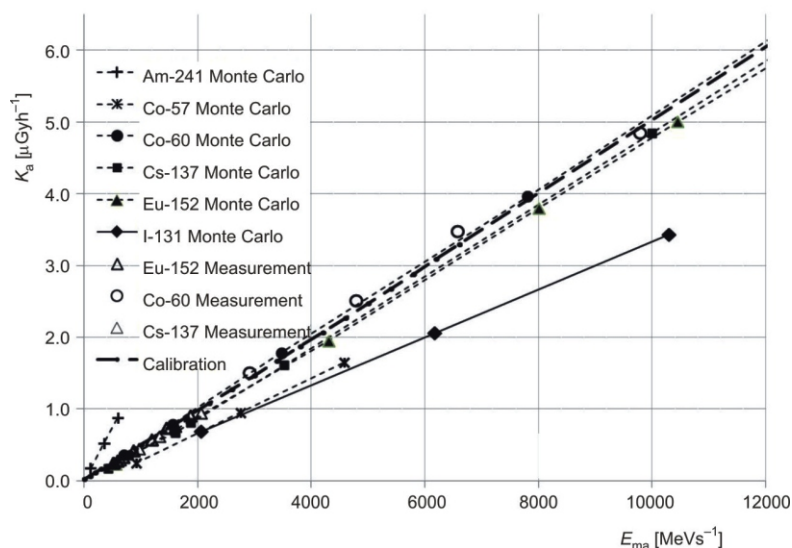


Figure 4. Monte Carlo simulation and measurements of the correlation between E_{ma} and K_a for 3" × 3" NaI(Tl) detector in the NBC calibration room for different nuclides

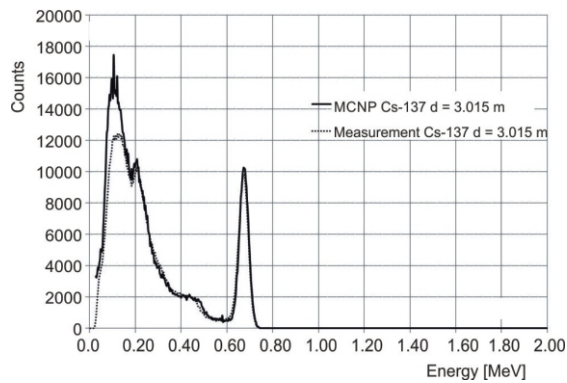


Figure 6. The $^{22} \text{Na}$ $^{22} \text{NaI(Tl)}$ spectra of ^{137}Cs 102.1 MBq measured and Monte Carlo simulated in the NBC calibration room at the detector – source distance of 3.015 m

small-volume plastic detectors used in environmental measurements. Two examples follow.

The first example gives the results from the calibration of $^{22} \text{Na}$ $^{22} \text{NaI(Tl)}$ in the NBC calibration room. The detector was calibrated from 125 nGyh^{-1} to $20 \text{ } \mu\text{Gyh}^{-1}$ with ^{137}Cs (102.5 MBq and 3.145 GBq) and ^{60}Co (100 MBq and 500 MBq) sources. Additionally, for the standard method, the air kerma was calculated from the simulated spectra and compared with the air kerma rate calculated from measured spectra. The measured and simulated spectrum for the detector-source distance of 3.015 m in the NBC calibration room with ^{137}Cs 102.1 MBq is shown in fig. 6.

Comparison of relative absorbed energy rates and air kerma rates based on both the MCNP calculation and measurements in three different distances and for ^{137}Cs and ^{60}Co are given in tab. 3. Similar data has

been received in all cases when simulated spectra were calculated and converted to the air kerma rates for such types of spectra.

The second example is shown in fig. 7. The air kerma rates in 32 points were measured at the NBC reference area in Vyškov, Czech Republic. This reference area is used for the airborne gamma-spectrometers verification and calibration. The individual ground points form a grid with a distance of 60 m from each other. The air kerma rates were calculated from the spectra taken by *in-situ* gamma-spectrometry measurements. The ORTEC HPGe GEM100P4-95 S/N 50-TP50739A was used and the calibration curve from fig. 3 was applied. The data of air kerma rates was compared with the air kerma rates determined from both natural nuclide activities and the data measured by the RSS Reuter&Stokes chamber. The air kerma rate calculated from the spectra of the ORTEC HPGe detector was $(89 \pm 4) \text{ nGyh}^{-1}$ on average at the whole reference area. The air kerma rate calculated from the natural nuclide activities plus ^{137}Cs surface activities in all 32 points was $(82 \pm 5) \text{ nGyh}^{-1}$ on average. The RSS air kerma rates were measured in 12 selected points by the RSS high pressure ion chamber. The RSS data was compensated by the contribution of cosmic radiation [14]. The value of $(99 \pm 5) \text{ nGyh}^{-1}$ on average was achieved.

CONCLUSION

The method of air kerma rate calibration described in this contribution was applied to different detector types NaI(Tl), HPGe and plastic scintillation detectors.

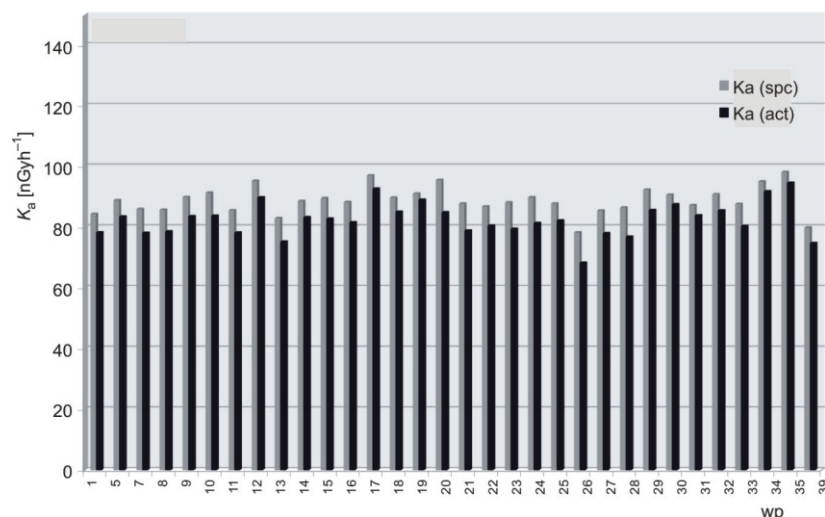


Figure 7. Air kerma rates K_a at 1 m above the ground (terrestrial component only) at the NBC reference area in Vyškov. $K_{a(\text{spc})}$ are the air kerma rates from the spectra of ORTEC HPGe GEM100P4-95 semiconductor detector calculated by the method described in this contribution; $K_{a(\text{act})}$ are the air kerma rates calculated from natural nuclide activities plus the ^{137}Cs surface activity

Table 3. Comparison of air kerma rates from spectra measured by the $^{22} \text{Na}$ $^{22} \text{NaI(Tl)}$ detector with values calculated in Monte Carlo simulated spectra (NBC calibration room)

Source	Source-detector distance [m]	$E_{\text{ma (meas)}} [\text{MeVs}^{-1}]$	$E_{\text{ma (MCNP)}} [\text{MeVs}^{-1}]$	$K_{a(\text{meas})} [\mu\text{Gyh}^{-1}]$	$K_{a(\text{MCNP})} [\mu\text{Gyh}^{-1}]$	[%]
^{137}Cs	3.015	2588	2687	3.79	3.94	-3.8
^{137}Cs	5.017	1083	1065	1.55	1.53	+1.3
^{60}Co	6.014	863	827.6	1.23	1.18	+4.2

All calibrations were verified by Monte Carlo simulations in different calibration conditions as well as compared with results of the Reuter&Stokes RSS high pressure ion chambers.

The method of calibration described in this contribution works well for a wide range of energies, *i. e.* environmental gamma-ray spectra from some tens of keV to 3 MeV overlapped with man-made nuclide spectra with energies higher than 300 keV.

It was proved that this approach can be used for calibrating small symmetrical detectors for the measurement of air kerma rates from low level background of 26 nGyh^{-1} up to $50 \text{ } \mu\text{Gyh}^{-1}$.

This calibration method showed energy independence in the tested energy ranges in all cases.

Uncertainties of calibrations were up to 10 %, which is acceptable for the intended detectors application in portable, mobile and airborne systems. The measurement uncertainties of obtained results were about 7 % which agrees with the expectations [15, 16]

The method was also tested to for standalone ^{241}Am (59.5 keV), ^{57}Co (122 keV), ^{131}I (364 keV) and other spectra only with energies in a range below 400 keV, see fig. 4.

This area calls for detailed investigation because the reliable results have not been achieved for low energy nuclides. The conversion factors shall be needed in case of low energy nuclides. Also, the calibration of non-symmetrical detectors should be investigated in the future.

Among others, the method is characterized by a couple of advantages. The conversion of the non-air kerma rate to the air kerma rate in detectors was eliminated, energy dependence was nearly eliminated and the dead time (DT) was involved in the calibration when it is not auto-corrected by the spectrometer.

ACKNOWLEDGEMENT

This study was supported by institutional funding from the Ministry of the Interior of the Czech Republic (project VI20172020104).

AUTHORS CONTRIBUTIONS

The idea of this contribution was proposed by M. Ohera who also processed the data and calculated Monte Carlo simulation. D. Sas provided all sources and technical support at NBC Defence Institute and P. Sladek provided many NaI(Tl) detectors, was also concerned in MCA development and together with D. Sas participated in measurements.

REFERENCES

[1] Gouda, M. M., Calibration of NaI (Tl) Cylindrical Detector Using Axially Shifted Radioactive Cylindrical Source, *Nucl Technol Radiat*, 34 (2019), 4, pp. 353-360

[2] Mihaljević, N. N., *et al.*, A Mathematical Model of Semiconductor Detector Gamma Efficiency Calibration for Rectangular Cuboid (Brick-shape) Sources. *Nucl Technol Radiat*, 33 (2018), 2, pp. 139-149

[3] Beck, H. L., *et al.*, Spectrometric Techniques for Measuring Environmental Gamma Radiation, HASL-150, Health and Safety Laboratory, New York, US AEC, 1972

[4] Beck, H. L., *et al.*, In situ Ge(Li) and NaI(Tl) Gamma-Ray Spectrometry HASL, Health and Safety Laboratory, New York, US, AEC, 1973

[5] Grasty, R. L., *et al.*, Calibration of a 7.6 cm \times 7.6 cm (3 inch \times 3 inch) Sodium Iodide Gamma Ray Spectrometer for Air Kerma Rate, *Radiat. Prot. Dosimetry*, 94 (2001), 4, pp. 309-316

[6] Tojo, T., A Method of Exposure-Dose-Rate Measurement with a NaI(Tl) Crystal, *Nuclear Instruments and Methods*, 205 (1983), 3, pp. 517-524

[7] Čechak, T., *et al.*, Spectra Processing in Airborne Gamma-ray Spectrometry Using ENMOS Detection System. Technical University of Prague, Faculty of Nuclear Science and Technical Engineering, Prague, May 1994

[8] Kluson, J., *In-situ* Gamma Spectrometry in Environmental Monitoring, *Applied Radiation and Isotopes*, 68 (2010), 4-5, pp. 529-535

[9] Kluson, J., Environmental Monitoring and In-Situ Gamma Spectrometry, *Radiation Physics and Chemistry*, 61 (2001), 3-6, pp. 209-216

[10] Hulka, J., *et al.*, Evaluation of Detector Responses in Extremely Low Gamma Background Using Innovated Technology of Low Background Chamber at SURO, Certificated Method (in Czech), National Radiation Protection Institute (SURO), Prague, 2015

[11] Chichester, D. L., *et al.*, Photon Dosimetry Using Plastic Scintillators in Pulsed Radiation Fields – Art. No. 65401K, Proceedings of SPIE – The International Society for Optical Engineering, 6540. 10.1117/12.722929, USA, April 2007

[12] Shultis, J. K., Faw, R. E., AN MCNP PRIMER, Dept. of Mechanical and Nuclear Engineering Kansas State University Manhattan, KS 66506, 2004-2006

[13] Skala, L., SW GAMWIN, User Guide, Nuvia CZ, a.s. Trebic, Czech Republic, 2015

[14] Sato, T., Analytical Model for Estimating Terrestrial Cosmic Ray Fluxes Nearly Anytime and Anywhere in the World: Extension of PARMA/EXPACS, PLOS ONE, 10, e0144 679, doi:10.1371/journal.pone.0144679, <http://journals.plos.org/plosone/article?id=10.1371/journal.pone.0144679>, 2015

[15] Lazarević, Z., *et al.*, A Novel Approach for Temperature Estimation in Squirrel-Cage Induction Motor Without Sensors, 1999, *IEEE Transactions on Instrumentation and Measurement*, 48 (1999), 3, pp. 753-757

[16] Osmokrović, P., *et al.*, Investigation of the Optimal Method for Improvement of the Protective Characteristics of Gas-Filled Surge Arresters – With/Without the Built-In Radioactive Sources, *IEEE Transactions on Plasma Science*, 30 (2002), 5 I, pp. 1876-1880

Received on September 16, 2020

Accepted on January 13, 2021

Марцел ОХЕРА, Данијел САС, Петрж СЛАДЕК

КАЛИБРАЦИЈА СПЕКТРОМЕТРИЈСКИХ ДЕТЕКТОРА ЗА ЈАЧИНУ КЕРМЕ ВАЗДУХА У МОНИТОРИНГУ ЖИВОТНЕ СРЕДИНЕ

Спектрометријски системи, посебно они засновани на NaI(Tl) и HPGe детекторима, користе се за идентификацију нуклида и прорачун њихових активности при мерењу тла и мониторингу ваздуха. Одређивање јачине керме ваздуха такође је веома важно за мерења у животној средини. У таквим случајевима детекторе треба калибрисати за јачину керме ваздуха у $\mu\text{Gy h}^{-1}$ или mGy h^{-1} . Једноставна калибрација NaI(Tl), HPGe као и пластичних детектора за ниске нивое керми у ваздуху, представљени су у овом раду.

Калибрација се заснива на упоређивању јачине релативне апсорбоване енергије у детекторима (MeVs^{-1}) израчунате из спектра, са јачинама ваздушне керме израчунатим Монте Карло симулацијом и допунским подацима из јонске коморе високог притиска RSS Reuter&Stokes. Овом методом такође се елиминише конверзија јачина неваздушних керми кристала у јачине ваздушне керме. Три различите врсте малих цилиндричних детектора калибрисане су за јачине ваздушне керме од позадинских $26 \mu\text{Gy h}^{-1}$ до неколико десетина mGy h^{-1} , у енергетском опсегу до максималне енергије од 3 MeV. Представљени су резултати калибрација NaI(Tl) димензија $3'' \times 3''$, HPGe детектора и малог пластичног детектора (направљеног од полистирена), укључујући неке примере мерења у животној средини.

Кључне речи: калибрација јачине керме у ваздуху, NaI(Tl), HPGe и пластични детектор,
Монте Карло симулација
